Since January 2020 Elsevier has created a COVID-19 resource centre with free information in English and Mandarin on the novel coronavirus COVID-19. The COVID-19 resource centre is hosted on Elsevier Connect, the company's public news and information website.

Chemosphere 289 (2022) 133213

Contents lists available at ScienceDirect

Chemosphere

journal homepage: www.elsevier.com/locate/chemosphere

Application of activated carbon functionalized with graphene oxide for efficient removal of COVID-19 treatment-related pharmaceuticals from water

Eduarda Freitas Diogo Januário [a], Yasmin Jaqueline Fachina [a], Gessica Wernke [a], Gabriela Maria Matos Demiti [a], Laiza Bergamasco Beltran [b], Rosângela Bergamasco [a], Angélica Marquetotti Salcedo Vieira [c,*]

[a] State University of Maringá, Department of Chemical Engineering, Maringá, 87020-900, Paraná, Brazil
[b] State University of Maringá, Graduate Program in Food Science, Maringá, 87020-900, Paraná, Brazil
[c] State University of Maringá, Department of Food Engineering, Maringá, 87020-900, Paraná, Brazil

HIGHLIGHTS

- Development of an efficient and innovative material for pharmaceuticals adsorption.
- GAC-GO obtained $q_{máx}$ of 37.65 and 62.43 mg g^{-1} for chloroquine and dipyrone adsorption.
- The removal of chloroquine, dipyrone, methylene blue, 2,4-D and triclosan were evaluated.
- Synergistic effects were proposed in the synthetic mixture.

GRAPHICAL ABSTRACT

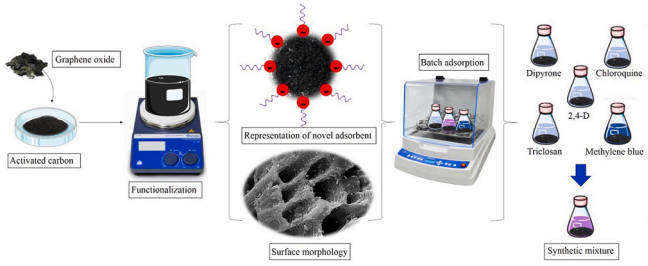

ARTICLE INFO

Handling Editor: Yongmei Li

Keywords:
Pharmaceuticals
Covid-19
Adsorbent functionalization
Synthetic mixture
Wastewater treatment

ABSTRACT

Currently, the COVID-19 pandemic has been increasing the consumption of some drugs, such as chloroquine (CQN) and dipyrone (DIP), which are continuously discharged into water resources through domestic sewage treatment systems. The presence of these drugs in water bodies is worrisome due to their high toxicity, which makes crucial their monitoring and removal, especially by means of advanced technologies. Given this scenario, a new adsorbent material was synthesized through the combination of babassu coconut activated carbon and graphene oxide (GAC-GO). This study was evaluated in batch adsorption processes, aiming at the treatment of water contaminated with CQN and DIP. Characterization analyzes using physicochemical and spectroscopic techniques indicated that the GAC-GO functionalization was successfully performed. The equilibrium time of the adsorption process was 18 and 12 h for CQN and DIP, respectively. Kinetic and isothermal data better fitted to pseudo-second-order and Langmuir models for both drugs. Thermodynamic parameters showed that the process is endothermic and the maximum adsorption capacities of CQN and DIP were 37.65 and 62.43 mg g^{-1}, respectively, both at 318 K. The study of the effect of ionic strength, which simulates a real effluent, demonstrated that the synthesized adsorbent has potential application for the treatment of effluents. Furthermore, satisfactory removal rates were verified for the removal of other contaminants in both simple solutions and synthetic mixtures, evidencing the versatile profile of the adsorbent.

* Corresponding author.
E-mail address: amsvieira@uem.br (A.M.S. Vieira).

https://doi.org/10.1016/j.chemosphere.2021.133213
Received 9 October 2021; Received in revised form 16 November 2021; Accepted 6 December 2021
Available online 7 December 2021

1. Introduction

The COVID-19 pandemic is one of the greatest threats that humanity has ever faced, in which the virus has spread rapidly around the world (Yunus et al., 2020). Thus, some studies raise awareness about water quality, since wastewater has been overloaded with persistent and organic due to the excessive use of disinfectants, antibacterials and pharmaceuticals (Elsaid et al., 2021; Feizizadeh et al., 2021). Chloroquine (CQN) has been used in some countries due to its probable benefits on control the infection caused by COVID-19 (Bagheri Novir and Aram, 2020; Gautret et al., 2020; Noureddine et al., 2021). In addition, dipyrone (DIP) has been also intensively used for analgesia and fever control during the symptomatic phase of the disease (Quesada et al., 2019a; Rivera-Utrilla et al., 2013).

It is noteworthy that approximately 33% of these drugs are excreted after oral administration, wherein conventional water treatment methods are not able to completely remove these contaminants. That being said, the application of advanced methods becomes crucial (Andrade et al., 2022; Januário et al., 2021a). The adsorption process stands out as a promising technique for the removal of organic contaminants from water due to its high efficiency, process simplicity, low cost and ecological feasibility (Lin et al., 2017; Luciano et al., 2020).

Graphene oxide (GO) is a material widely applied in adsorption processes by virtue of its excellent performance, porous structure and abundance of oxygenated functional groups, which allow the formation of strong interactions with organic contaminants (Guerra et al., 2021; Rostamian and Behnejad, 2018). However, the GO use can become an expensive and disadvantageous alternative given its synthesis process and ease in forming clusters (Li et al., 2021). Thus, an interesting alternative to this issue is the aggregation of GO properties in other materials, aiming the development of new adsorbents (Wernke et al., 2021).

In this sense, activated carbons stand out since they are advantageous materials for adsorption. They are versatile, efficient and have low costs of obtaining, being commonly obtained from industrial waste. Many studies have reported the activated carbon synthesis from several biodegradable alternative materials, such as bananas peels (Marichelvam and Azhagurajan, 2018), nutshells (Nazari et al., 2016), rice husks (de Luna et al., 2013) and babassu coconut shells (Vidovix et al., 2019a).

Therefore, considering the GO excellent properties and the potential application of activated carbons in adsorptive processes, the present study aimed to develop a new adsorbent by combining GO with activated carbon from babassu bark. This adsorbent was synthesized and evaluated in batch adsorption processes, aiming at the treatment of water contaminated with CQN and DIP pharmaceuticals.

2. Materials and methods

2.1. Adsorbate

The CQN (Farmácia Catanduvas, Astorga, Paraná, Brazil) and DIP (Medfórmula, Maringá, Paraná, Brazil) properties are described in Table S1. Both drugs used were 95% purity. As regards the adsorption tests, the contaminants were diluted in deionized water, in which their concentrations were determined in a UV–vis spectrophotometer (HACH DR 5000) at wavelengths of 343 and 258 nm for CQN and DIP, respectively.

2.2. Adsorbent preparation

The GO synthesis was performed according to the modified Hummers' method (Hummers and Offeman, 1958) described by Yamaguchi et al. (2016). Thereafter, the GO nanosheets were dispersed in deionized water using an ultrasonic homogenizer, in order to obtain a GO aqueous solution. Granular activated carbon (GAC) obtained from babassu coconut shells was donated by Purific (Maringá, Paraná, Brazil). Concerning the preparation of the new adsorbent, the functionalization and thermal treatment have been carried out. The functionalization step was adapted from Wernke et al. (2021) in which GAC and GO were mixed at a ratio of 1:1 (m/V) in a shaker with temperature control (150 rpm at 423 K) until the complete evaporation of the aqueous phase. Afterward, the activated charcoal functionalized with GO was oven-dried at 373 K for 24 h. The heat treatment step followed the methods described by Vidovix et al. (2019a), in which the adsorbent was heated at high temperatures (623–723 K) in a muffle. The new adsorbent was sieved in the size range of 300 μm in a set of meshes in a vibrating table (BT-001). Finally, it was named GAC-GO, being evaluated for its adsorption potential.

2.3. Adsorbent characterization

Scanning electron microscopy analysis (SEM, Quanta FEI – 250) was performed to evaluate the GAC-GO surface morphology, generated by topographic contrast. The zeta potential determined the surface charges of the material (Beckman Coulter – Delsa™ NanoC). For this purpose, the samples' pH dispersed in deionized water was adjusted with 0.1 M of HCl and NaOH solutions. Fourier transform infrared spectroscopy analysis (FTIR, Vertex 70v, Bruker, Germany) was used to determine the functional groups present in the adsorbent. Finally, X-ray diffraction analysis (XRD, AXSD8 Advance, Bruker) defined the structure of GAC-GO. The mean particle diameter (d) was estimated by Scherrer's Equation (Equation (1)).

$$d = \frac{0,89\lambda}{B cos\theta_B} \quad (1)$$

where 0.89 is the constant related to the spherical approximation; λ refers to the radiation wavelength; B is the peak width at half height; and θ_B is the Bragg angle (Koch, 2007).

2.4. Adsorption experiments

CQN and DIP adsorption tests were carried out in batches and in duplicate, on a shaker table with temperature control (Tecnal TE – 4200) at 150 rpm. Accordingly, 20 mL of the contaminant solution at a concentration of 30 mg L^{-1} was used for the tests. First, the mass effect was investigated using 0.02, 0.03 and 0.04 g at 298 K for 24 h. Later, the effect of pH (4, 7, 10 and natural) was also analyzed. After determining the working mass and pH, the study of the effects caused by the ionic strength was performed. $MgCl_2$, NaCl and KCl at concentrations of 0.1 and 0.3 M were individually dissolved in the contaminant solutions and kept under stirring at 298 K for 24 h, in order to verify the influence of the free ions on the adsorption capacity.

Regarding the kinetic study, the contact time of the adsorbent with CQN and DIP was evaluated at 298 K for 28 h. In sequence, the pseudo-first-order (PFO) and pseudo-second-order (PSO) kinetic models were applied to the experimental data to understand the adsorption mechanisms. In addition, the intraparticle diffusion model described by Weber and Morris (1963) was also applied.

The adsorption isotherms were evaluated by varying the CQN and DIP concentrations from 5 to 100 mg L^{-1}, at three different temperatures (298, 308 and 318 K) with a predefined equilibrium time. The equilibrium data were fitted to the Langmuir and Freundlich models in order to assess the adsorbate/adsorbent interaction (Weber et al., 1991). The thermodynamic parameters (Gibbs Free Energy (ΔG°), Enthalpy (ΔH°) and Entropy (ΔS°)) were applied to analyze the spontaneity, viability and heat exchange of the adsorptive process (Anastopoulos and Kyzas, 2016).

At the end of each experiment, the samples were filtered on cellulose acetate membranes (UNIFIL) with an average pore size of 0.45 μm. Sequentially, the concentration was determined. Thus, the adsorption

capacity (q_e, mg g^{-1}) was calculated by Equation (2).

$$q_e = \frac{(C_0 - C_e)V}{m} \quad (2)$$

where C_0 and C_e are the initial and final contaminants concentration (mg L^{-1}), respectively; V is the solution volume (L); and m is the GAC-GO mass (g).

In addition to CQN and DIP, a dye (methylene blue, Synth, Diadema, São Paulo, Brazil), herbicide (2,4-dichlorophenoxyacetic (2,4-D), Nortox, Arapongas, Paraná, Brazil) and antibacterial (triclosan, Medfórmula, Maringá, Paraná, Brazil) adsorption were also evaluated using GAC-GO. They were assessed in both simple solutions and synthetic mixture, in order to simulate a real effluent and verify the adsorbent versatility. The adsorption tests were carried out for 24 h with 30 mg L^{-1} of the contaminant concentration, except for the methylene blue dye (20 mg L^{-1}). These experiments were carried under the same experimental conditions (298 K, 150 rpm, natural pH). The contaminants concentration was measured in a UV–Vis spectrophotometer, using a previously prepared standard curve at 665, 284 and 280 nm wavelengths for the methylene blue, 2,4-D and triclosan, respectively.

3. Results and discussion

3.1. Adsorbent characterization

Fig. 1 presents the characterization analyzes of the GAC-GO.

The micrograph of the GAC-GO obtained by SEM (Fig. 1 (A)) presents heterogeneous morphological characteristics since the pores are well defined, deep and distributed throughout the adsorbent surface. These characteristics are typical of GAC (Paixão et al., 2018; Vidovix et al., 2019a). The surface rough appearance proves the functionalization of the activated carbon with GO (Fachina et al., 2020). Furthermore, Figure S1 shows the GAC (A) and GAC-GO (B) micrographs at 3000 × magnification. It was possible to observe that GAC had an extremely porous surface and, after functionalization with GO, there was an irregular distribution of GO nanoparticles on the surface of GAC which, consequently, decreased the porosity of the biosorbent. This behavior was also reported by Wernke et al. (2021).

The GAC-GO zeta potential (Fig. 1 (B)) shows a predominance of negative charges in the pH range studied (7.73 to −35.41 mV). It was verified that the GAC-GO isoelectric point is close to 3, indicating that the adsorbent surface charge is positive at pH < 3 and negative at pH > 3. Figure S2 presents the zeta potential of GAC and GO, separately. It is possible to verify that GAC and GAC-GO have positive charges at pH 2 and tend to become more negative as pH increases. Furthermore, the highest negative charge density (−43.80 mV) was observed at pH 10. This behavior was similar to the zeta potential of the GO aqueous solution, confirming the GAC functionalization.

In the FTIR spectrum of the material (Fig. 1 (C)) it is possible to verify a large number of functional groups, characteristic of biosorbents and GO. Peak 3221 cm^{-1} corresponds to the elongation vibration of the hydroxyl groups (O—H) of the water molecules adsorbed by GAC-GO (Hacıosmanoğlu et al., 2019; Hoppen et al., 2019; Karkooti et al., 2018). The peaks located at 1554, 1393 and 1085 cm^{-1} are typical of charcoals synthesized from biomaterials and represent the carbonyl, ketone and ether groups, respectively (Vidovix et al., 2019a). The peak at 880 cm^{-1} is related to the ester groups and aromatic rings existing in GAC, due to the lignin present in the babassu coconut (Vieira et al., 2009). The functionalization of GAC with GO is confirmed in peak 1612 cm^{-1}, which refers to the C═O bond, suggesting the presence of carboxy groups, anhydrides and esters (Yamaguchi et al., 2016). Furthermore, peak 1064 cm^{-1} is related to C–O stretching vibration of the epoxy and hydroxyl groups of GO (Januário et al., 2020). Other peaks can be observed at 1459 and 1212 cm^{-1} which can be attributed to the vibration of the C═C bond and aromatic ether (Homem et al., 2019).

The XRD analysis (Fig. 1 (D)) allows to verify characteristic peaks of the precursor materials of the adsorbent. The peak at 2θ = 7.20° indicates the presence of GO, which corresponds to the aggregation of

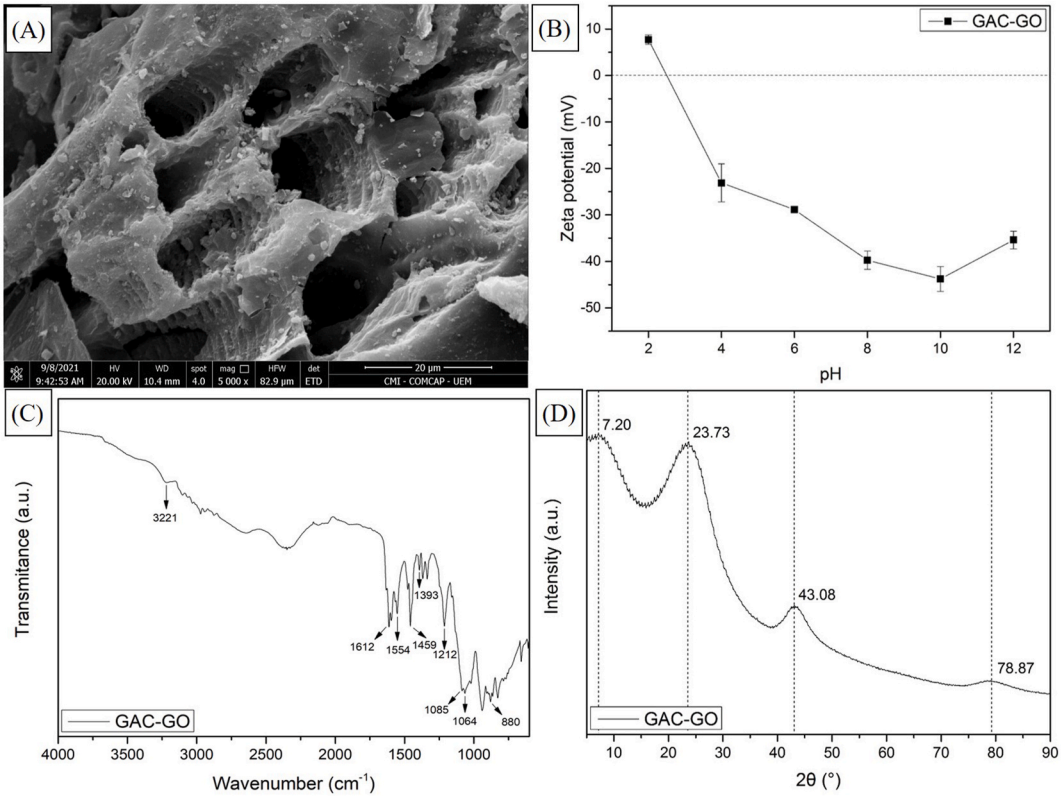

Fig. 1. SEM images (A), zeta potential (B), FTIR (C) and XRD analysis (D) of the GAC-GO.

functional groups on the surface of GAC, such as hydroxyl (–OH), carboxyl (–COOH), carbonyl (–C═O) and epoxy (–COC–) (de Souza et al., 2021). The 2θ = 23.73° peak refers to the cellulosic compounds present in amorphous materials. Vidovix et al. (2019a) also reported peaks near 2θ = 43.08° and 78.87°, which refer to GAC composition. In addition, the average diameter of the adsorbent was 3.24 nm. It is noteworthy that the diameter of GAC-GO is not uniform, due to its heterogeneous characteristic, as can be seen in the SEM images (Fig. 1 (A)).

3.2. Effect of mass

The effect of adsorbent dosage on the adsorption and removal capacity of CQN (A) and DIP (B) reported a similar behavior, since the 0.02, 0.03 and 0.04 g GAC-GO masses resulted in adsorption capacities of 25.06, 20.95 and 15.91 mg g^{-1} for CQN and 27.64, 20.01 and 15.09 mg g^{-1} for DIP, respectively. Concomitantly, there was an improvement in drug removal percentages by increasing the adsorbent mass, ranging from 78.76 to 100% and 86.63–94.61% for CQN and DIP, respectively. de Souza et al. (2021) reported that the adsorption capacity decreases in larger adsorbent masses due to the excess of unsaturated active sites, or the adsorbent material aggregation, which reduces the total surface area and increases the contaminant diffusion path. Thus, the subsequent tests were carried out using a mass of 0.03 g, as it obtained favorable conditions of adsorption and removal capacity (98.77 and 94.07% for CQN and DIP, respectively).

3.3. pH effect

The adsorption capacity of the drugs was evaluated at pH 4, 7, 10, and natural (i.e., 5.78 and 6.08 for CQN and DIP, respectively), as shown in Fig. 2.

It was verified that between pH 4 and 7, the adsorption capacity of CQN did not show great changes (18.39–19.41 mg g^{-1}). However, at pH 10 there was a drastic reduction in the adsorption capacity to 7.43 mg g^{-1}. This is due to the fact that CQN has a pKa of 8.76, which means that it is a weak acid and has a tendency to donate electrons (Poschet et al., 2020). Thus, at pH < pKa (between pH 4 and 7), CQN is in its non-ionic form (protonated). Consequently, the adsorption process cannot be explained by electrostatic interactions. This fact suggests that hydrogen bonds and π-interactions are the main mechanism of CQN adsorption onto GAC-GO. CQN presented negative charges at pH 10, as it is deprotonated, providing electrostatic repulsion between the CQN anions and the negatively charged surface of GAC-GO, as verified in the zeta potential analysis (item 3.1.) (Quesada et al., 2019b).

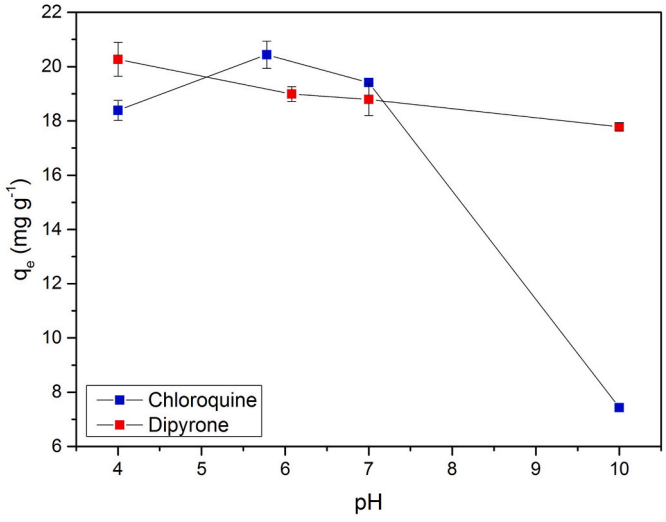

Fig. 2. pH effect on the adsorption capacity of DIP and CQN onto GAC-GO (C_0 = 30 mg L^{-1}, GAC-GO mass = 0.03 g, T = 298 K, contact time = 24 h, stirring velocity = 150 rpm).

As regards the DIP, it was verified that the adsorptive capacity did not present great changes in the evaluated pH range (17.78–20.27 mg g^{-1}). According to Modesto et al. (2021), the DIP has a pKa of 3.77, in which it is deprotonated above this value. However, DIP removal cannot be explained by electrostatic repulsion between the adsorbent and adsorbate since the GAC-GO adsorptive capacity was satisfactory. In addition, no change was reported with pH variation. According to Fachina et al. (2020), the low pH dependence indicates that the adsorption process is governed by weak interactions, such as hydrogen bonds and π-interactions. de Andrade et al. (2019) studied the DIP adsorption onto GO functionalized with iron and zinc oxide nanoparticles, wherein the adsorptive capacity was not influenced by the pH.

Thus, the results demonstrated that there was no necessity of pH correction for the following experiments, given the satisfactory adsorption capacity at natural pH for both drugs. This ensures practicality for the process, as well as cost reduction with chemical reagents.

3.4. Effect of ionic strength

A comparative study regarding the adsorption capacity of pure drugs and with $MgCl_2$, NaCl and KCl dissolved salts, at concentrations of 0.1 and 0.3 M, was carried out (Figure S3). This study allows to simulate a real effluent, provided the aqueous matrices have several compounds diluted in cationic and anionic forms, such as Mg^{+2}, Na^{+}, K^{+} and Cl^{-}. These compounds can change the adsorptive capacity and influence the hydrophobic and electrostatic interactions between the adsorbent and the drugs (Vidovix et al., 2019a; Zhang et al., 2019).

It was verified that the presence of all salts studied did not pronounced alter the adsorption capacity of the drugs, regardless of the concentration used, as it ranged from 21.03 to 21.27 mg g^{-1} for CQN (A), and 19.51–19.88 mg g^{-1} for DIP (B). Thus, the results demonstrated that van der Waals forces and hydrogen bonds are the key mechanisms that govern the pharmaceuticals adsorption onto GAC-GO, once the adsorption capacity was not affected by the presence of ions in the solution (Januário et al., 2021b). Therefore, this behavior suggests that the application of GAC-GO is advantageous for drug removal from wastewater.

3.5. Kinetic study

The kinetic study of CQN and DIP are shown in Fig. 3. It aimed to determine the adsorption capacity of drugs over time. It was verified that the process did not present expressive variations in the adsorption capacity in 18 h (19.83–20.57 mg g^{-1}) for CQN and in 12 h (19.45–20.01 mg g^{-1}) for DIP. Thus, the equilibrium was achieved as both curves reached a plateau, indicating that the adsorption and desorption processes occur simultaneously (de Souza et al., 2021). Kinetic data were fitted to the PFO and PSO models, whose parameters are shown in Table S2.

The kinetic behavior of the drugs has similarities that can be confirmed by the good fit of the two mathematical models to the experimental data, given the satisfactory correlation coefficients (R^2). However, the PSO model stands out for presenting a higher R^2 for CQN (0.982) and DIP (0.990). Moreover, the calculated adsorption capacity is in accordance with the parameters obtained experimentally (21.40 mg g^{-1} and 20.60 mg g^{-1} for CQN and DIP, respectively). This model suggests that the drugs adsorptive capacity is directly associated with the number of available active sites (Tran et al., 2017).

The Weber and Morris model (1963) was also fitted to kinetic data in order to understand the drug adsorption mechanisms. It can be seen in Fig. 3 (C) that intraparticle diffusion is not the only limiting step that controls the CQN and DIP adsorption, considering that the line does not reach the graph origin for both drugs, which indicates that the system

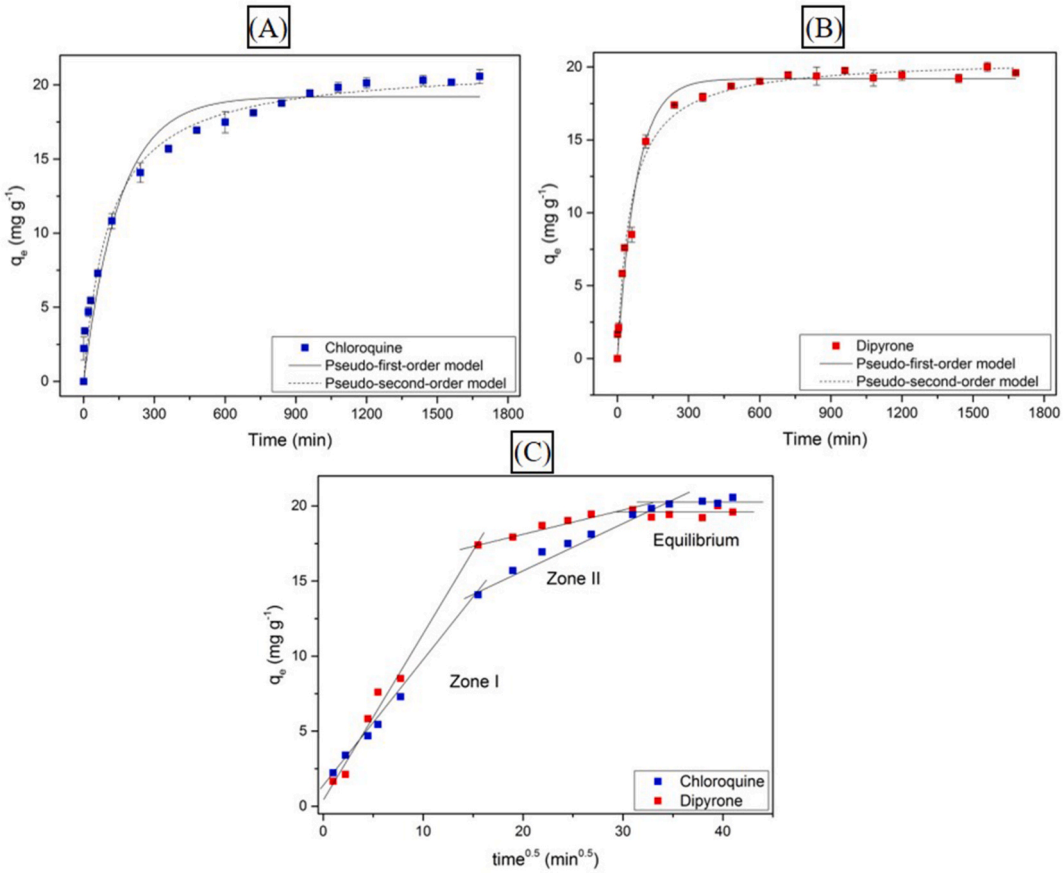

Fig. 3. Adsorption kinetic study of CQN (A) and DIP (B) onto GAC-GO with adjustments to the PFO and PSO, and intraparticle diffusion (C) models (C_0 = 30 mg L^{-1}, GAC-GO mass = 0.03 g, natural pH, T = 298 K, stirring velocity = 150 rpm).

has several steps (i.e., water phase transport, film diffusion, intraparticle diffusion and surface reaction) (de Souza et al., 2021). It is noteworthy that the first and last stages occur slowly and can be disregarded (Lladó et al., 2016).

Thus, zone I demonstrates that CQN and DIP are transported across the boundary layer of GAC-GO. Meanwhile, zone II refers to intraparticle diffusion, in which drug molecules are transported to the adsorbent pores (Quesada et al., 2019b). The values of C (Table S3), determined for zone I and II, are associated with the transfer resistance of the adsorbate to the adsorbent (Hiew et al., 2019). Thus, transport by film diffusion was faster when compared to transport by intraparticle diffusion, resulting in a higher diffusion constant (K_{dif}) in zone I. Finally, zone III is defined by the horizontal line, indicating that the equilibrium of the adsorptive process was achieved (Wu et al., 2009). Therefore, the presence of the three linear zones suggests that the adsorption process of CQN and DIP onto GAC-GO is driven by the described diffusion mechanisms.

3.6. Adsorption isotherms

Aware that the temperature is one of the factors that most influence the adsorption of contaminants, the CQN and DIP adsorption onto GAC-GO was investigated at 298, 308 and 318 K. The experimental data were adjusted to the Langmuir and Freundlich models (Table S3), and the evaluation of the best model was determined by comparing the correlation coefficients (R^2).

Fig. 4 demonstrate that both Langmuir and Freundlich isotherm models presented a well fit to the experimental data for the two contaminants. However, in both cases, the R^2 values for the Langmuir model were higher than those obtained by Freundlich at the three temperatures studied. It suggests that the adsorption of CQN and DIP onto GAC-GO occurs homogeneously and in a monolayer. Therefore, there is no interaction between the adsorbed molecules of the pharmaceuticals (Foo and Hameed, 2010; Langmuir, 1917).

The maximum adsorption capacity calculated by the Langmuir model was 37.65 mg g^{-1} for CQN and 62.43 mg g^{-1} for DIP, at 318 K. Dada et al. (2021) found the maximum adsorption capacity at 313 K for CQN, and a better fit to the Langmuir model. This evidences that in the 310–320 K range, the highest CQN adsorption in activated carbon-based adsorbent materials occurs.

Springer et al. (2016) and de Andrade et al. (2019) also found maximum adsorption capacities for DIP in the 300–320 K range. In addition, the experimental data were better fitted to the Langmuir model in both studies, proving which, such as CQN, the adsorption of dipyrone occurs mostly in monolayer (i.e., with identical binding energies and without interaction between the adsorbed molecules).

3.7. Thermodynamics parameters

In order to better understand the adsorption mechanism, thermodynamic parameters such as Gibbs free energy (ΔG°), enthalpy (ΔH°) and entropy (ΔS°) were investigated, in which their results are shown in Table 1. Both CQN and DIP adsorption occurred favorably and spontaneously ($\Delta G^\circ < 0$) at all evaluated temperatures. The negative values of Gibbs free energy indicate that the system does not require external energy during the process (Cusioli et al., 2021).

The positive value of ΔH° shows that the process occurs endothermically, which means that the increase in temperature positively influences the adsorption of CQN and DIP onto GAC-GO (Barbosa De Andrade et al., 2020). However, as can be seen in the isotherms (item

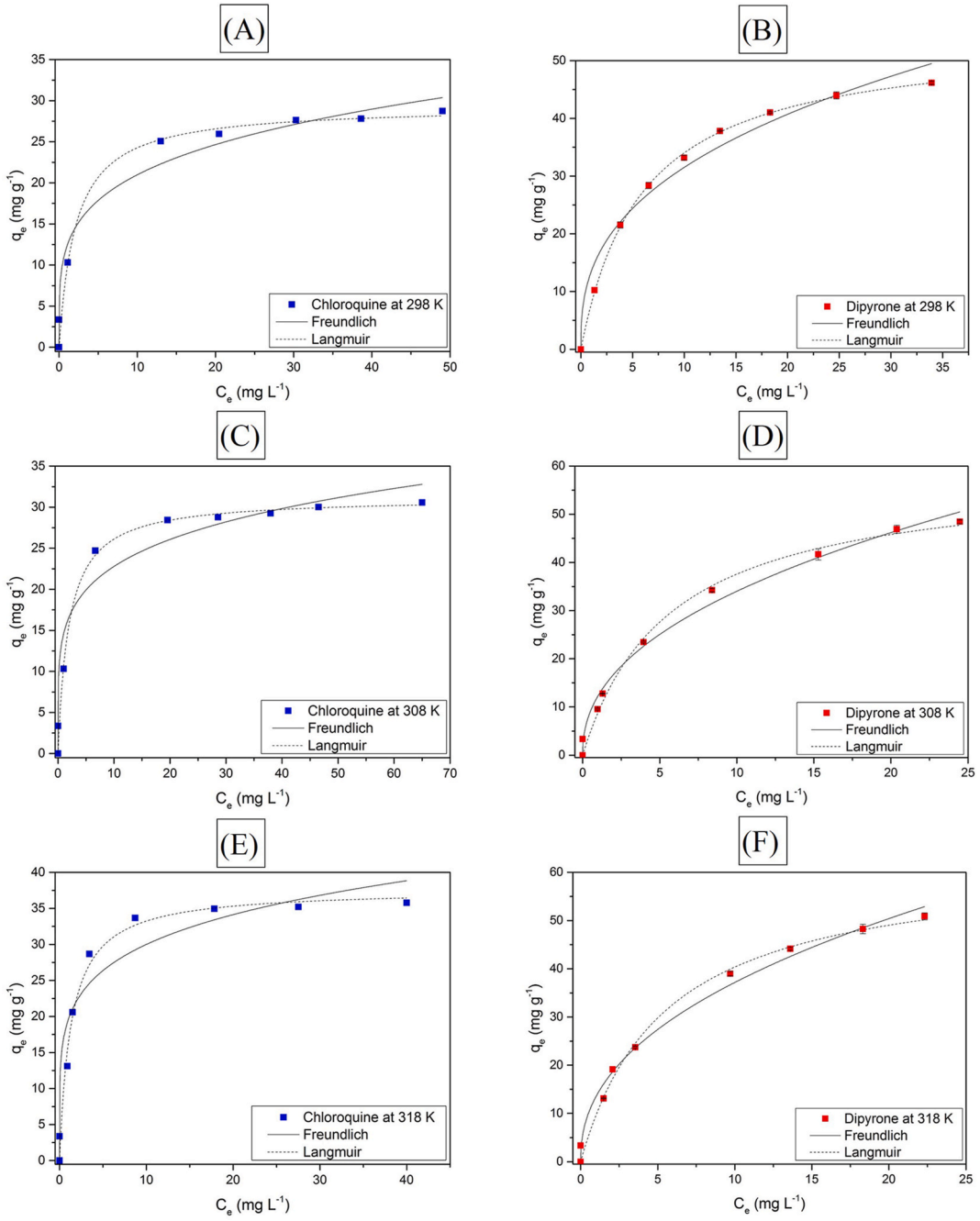

Fig. 4. Freundlich and Langmuir models fitted to the experimental data (GAC-GO mass = 0.03 g, T = 298 K, natural pH, stirring velocity = 150 rpm).

Table 1
Thermodynamic parameters of CQN and DIP adsorption onto GAC-GO.

Thermodynamic parameters							
		Chloroquine			Dipyrone		
		298 K	308 K	318 K	298 K	308 K	318 K
ΔG° (KJ mol^{-1})	$\Delta G^\circ = -RT\ln K_C$	−29.569	−30.767	−32.764	−27.233	−28.279	−29.271
ΔH° (KJ mol^{-1})	$\ln K_C = \frac{\Delta S}{R} - \frac{\Delta H}{R.T}$		17.90			3.14	
ΔS° (KJ mol^{-1} K^{-1})			0.159			0.102	

3.6.), the adsorptive process was similar behavior even with temperature variation since it did not cause pronounced changes in the adsorption capacity. The positive value of ΔS° indicates that the interaction between contaminants and GAC-GO occurred randomly at the solid-liquid interface.

3.8. Competitive adsorption in synthetic mixture

Fig. 5 (A) shows the contaminants adsorption onto GAC-GO separately. It is possible to verify that the adsorbent material proved to be efficient for adsorption, once the removal rate was greater than 90% for all analyzed contaminants. Therefore, the adsorption of various pollutants in simple solutions is related to the ability of GAC-GO to act in water and sewage treatment.

It is noteworthy that there was an interaction between the negatively charged surface of the adsorbent and the dye cations, suggesting that the adsorption of methylene blue occurred by electrostatic interactions (Vidovix et al., 2019b). This result may also be related to the GAC-GO surface area, given the porous characteristic of the adsorbent (Vidovix et al., 2019a). The removal rate of the methylene blue was 91.93%, while its adsorption capacity was 11.81 mg g^{-1}, being lower than the other contaminants due to dye initial concentration (20 mg g^{-1}).

Triclosan adsorption is explained by π-interactions and hydrogen bonds, since it is a weak acid (pKa 7.9) and it is in its protonated form at natural pH (Ma et al., 2019). The 2,4-D adsorption process was also governed by weak interactions (e.g., π-interactions and hydrogen bonds). This is due to the fact that despite having a pKa of 2.98, it presented a high adsorption capacity (20.59 mg g^{-1}) (Han et al., 2010). In summary, adsorption of triclosan and 2,4-D showed the same behavior as CQN and DIP, respectively.

However, in real effluents, there are several dissolved contaminants that can influence the adsorption mechanisms (Quesada et al., 2021). Thus, the adsorbent behavior in the treatment of the five contaminants altogether was investigated, so that this synthetic mixture simulates a real effluent. The UV–Vis spectrum of the mixture is shown in Fig. 5 (B), as well as the coloration before and after the adsorptive process. The process had 81.90% average removal of contaminants, proving the adsorbent effectiveness for the treatment of complex effluents. These results suggest that synergistic effects occurred in the synthetic mixture, demonstrating the necessity of evaluating the composition of real aqueous matrices.

3.9. Interaction mechanisms

The possible adsorption mechanisms were proposed in Fig. 6. According to the study of the pH effect and ionic strength effect, it is possible to suggest that hydrogen bonds and π-interactions govern the adsorption process of both contaminants onto GAC-GO. Furthermore, the adsorbent has aromatic rings and functional groups in its structure, due to the GO functionalization (Januário et al., 2021c), which also shows a preference for hydrogen bonds and π-interactions between the adsorbent and the contaminants.

In summary, the interactions between the oxygenated groups of GAC and the hydrogenated functional groups of CQN and DIP can be explained by hydrogen bonds. Meanwhile, the π-interactions are justified by the presence of aromatic rings in CQN and DIP, which interact with the conjugated π domains of GAC-GO (Januário et al., 2021b). Both interactions can be considered weak, being controlled by physical forces (Ali et al., 2012). Enthalpy change values of 17.90 and 3.14 kJ mol^{-1} for CQN and DIP, respectively, also confirm the physisorption process characteristic.

4. Conclusion

The presence of pharmaceuticals residues in wastewater is a global preoccupation since it can cause negative impacts on aquatic organisms and human health. The COVID-19 pandemic may have aggravated this problem even further due to the increased consumption of drugs worldwide. In addition, conventional water treatments do not effectively remove these compounds. Therefore, the present work proposed an alternative treatment for CQN and DIP removal by means of the new adsorbent material, obtained through the functionalization of GAC with GO. The synthesized adsorbent showed satisfactory characteristics for the adsorption of CQN and DIP from water, as its well-defined pores facilitate the adsorption of these contaminants. Equilibrium time was reached at 18 and 12 h, for CQN and DIP, respectively. The PSO and Langmuir models better fitted the kinetic and isothermal data for both contaminants. Thermodynamic parameters infer that the process is controlled by physical forces, suggesting that the adsorption is favorable, spontaneous and endothermic. The simulation of a real effluent using dissociated ions did not reduce the efficiency of the adsorption process, evidencing the applicability of GAC-GO. In the synthetic mixture, the synergistic effect of the compounds reduced the adsorbent removal efficiency. However, it still showed a satisfactory outcome (81.90%), proving the adsorbent effectiveness in treating complex effluents. Therefore, GAC-GO has the potential to remove several contaminants in effluent and contaminated water treatment processes.

Author contributions

Eduarda Freitas Diogo Januário: Conceptualization; Methodology; Formal analysis; Investigation; Writing-reviewing and editing. Yasmin Jaqueline Fachina: Formal analysis; Writing – original draft; Visualization; Investigation; Validation. Gessica Wernke: Conceptualization; Methodology; Visualization; Project administration. Gabriela Maria Matos Demiti: Conceptualization; Validation; Formal analysis;

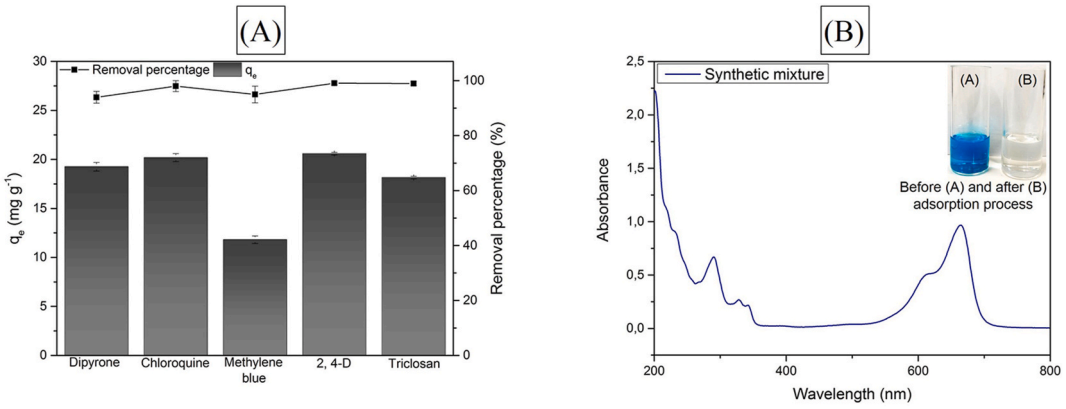

Fig. 5. Adsorption capacity and contaminants removal percentage in simple solutions (A); and treatment performance in synthetic mixture (B).

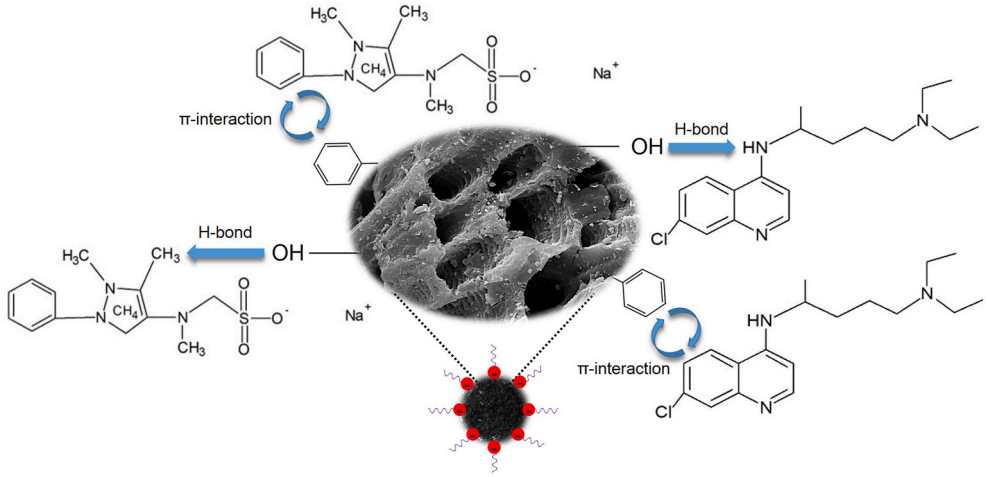

Fig. 6. Possible interaction mechanisms between the adsorbent and the contaminants.

Investigation. Laiza Bergamasco Beltran: Formal analysis; Investigation; Writing – review & editing; Visualization. Rosângela Bergamasco: Resources; Formal analysis. Angélica Marquetotti Salcedo Vieira: Resources; Supervision.

Declaration of competing interest

The authors declare that they have no known competing financial interests or personal relationships that could have appeared to influence the work reported in this paper.

Acknowledgements

This work was supported by the National Council for Scientific and Technological Development (CNPq) and Higher Education Personnel Improvement Coordination (CAPES), Financing Code 001. The authors also thank the Complex of Research Support Center (COMCAP) of the State University of Maringá (UEM) for the characterization analysis.

Appendix A. Supplementary data

Supplementary data to this article can be found online at https://doi.org/10.1016/j.chemosphere.2021.133213.

References

Ali, I., Asim, M., Khan, T.A., 2012. Low cost adsorbents for the removal of organic pollutants from wastewater. J. Environ. Manag. 113, 170–183. https://doi.org/10.1016/j.jenvman.2012.08.028.

Anastopoulos, I., Kyzas, G.Z., 2016. Are the thermodynamic parameters correctly estimated in liquid-phase adsorption phenomena? J. Mol. Liq. https://doi.org/10.1016/j.molliq.2016.02.059.

Andrade, M.B., Santos, T.R.T., Guerra, A.C.S., Silva, M.F., Demiti, G.M.M., Bergamasco, R., 2022. Evaluation of magnetic nano adsorbent produced from graphene oxide with iron and cobalt nanoparticles for caffeine removal from aqueous medium. Chem. Eng. Process. - Process Intensif. 170, 108694. https://doi.org/10.1016/j.cep.2021.108694.

Bagheri Novir, S., Aram, M.R., 2020. Quantum mechanical simulation of Chloroquine drug interaction with C60 fullerene for treatment of COVID-19. Chem. Phys. Lett. https://doi.org/10.1016/j.cplett.2020.137869.

Barbosa De Andrade, M., Sestito Guerra, A.C., Tonial Dos Santos, T.R., Cusioli, L.F., De Souza Antônio, R., Bergamasco, R., 2020. Simplified synthesis of new GO-α-γ-Fe2O3-Sh adsorbent material composed of graphene oxide decorated with iron oxide nanoparticles applied for removing diuron from aqueous medium. J. Environ. Chem. Eng. https://doi.org/10.1016/j.jece.2020.103903.

Cusioli, L.F., Quesada, H.B., Barbosa de Andrade, M., Gomes, R.G., Bergamasco, R., 2021. Application of a novel low-cost adsorbent functioned with iron oxide nanoparticles for the removal of triclosan present in contaminated water. Microporous Mesoporous Mater. https://doi.org/10.1016/j.micromeso.2021.111328.

Dada, A.O., Inyinbor, A.A., Bello, O.S., Tokula, B.E., 2021. Novel plantain peel activated carbon–supported zinc oxide nanocomposites (PPAC-ZnO-NC) for adsorption of chloroquine synthetic pharmaceutical used for COVID-19 treatment. Biomass Convers. Biorefin. https://doi.org/10.1007/s13399-021-01828-9.

de Andrade, M.B., Guerra, A.C.S., dos Santos, T.R.T., Mateus, G.A.P., Bergamasco, R.N., 2019. Innovative adsorbent based on graphene oxide decorated with Fe2O3/ZnO nanoparticles for removal of dipyrone from aqueous medium. Mater. Lett. https://doi.org/10.1016/j.matlet.2018.11.168.

de Luna, M.D.G., Flores, E.D., Genuino, D.A.D., Futalan, C.M., Wan, M.W., 2013. Adsorption of Eriochrome Black T (EBT) dye using activated carbon prepared from waste rice hulls-Optimization, isotherm and kinetic studies. J. Taiwan Inst. Chem. Eng. https://doi.org/10.1016/j.jtice.2013.01.010.

de Souza Antônio, R., Guerra, A.C.S., de Andrade, M.B., Nishi, L., Baptista, A.T.A., Bergamasco, R., Vieira, A.M.S., 2021. Application of graphene nanosheet oxide for atrazine adsorption in aqueous solution: synthesis, material characterization, and comprehension of the adsorption mechanism. Environ. Sci. Pollut. Res. https://doi.org/10.1007/s11356-020-10693-4.

de Souza, R.M., Quesada, H.B., Cusioli, L.F., Fagundes-Klen, M.R., Bergamasco, R., 2021. Adsorption of non-steroidal anti-inflammatory drug (NSAID) by agro-industrial by-product with chemical and thermal modification: adsorption studies and mechanism. Ind. Crop. Prod. https://doi.org/10.1016/j.indcrop.2020.113200.

Elsaid, K., Olabi, V., Sayed, E.T., Wilberforce, T., Abdelkareem, M.A., 2021. Effects of COVID-19 on the environment: an overview on air, water, wastewater, and solid waste. J. Environ. Manag. https://doi.org/10.1016/j.jenvman.2021.112694.

Fachina, Y.J., Andrade, M.B., de Guerra, A.C.S., Santos, T., Bergamasco, R., Vieira, A.M.S., 2020. Graphene oxide functionalized with cobalt ferrites applied to the removal of bisphenol A: ionic study, reuse capacity and desorption kinetics. Environ. Technol. https://doi.org/10.1080/09593330.2020.1830183.

Feizizadeh, B., Omarzadeh, D., Ronagh, Z., Sharifi, A., Blaschke, T., Lakes, T., 2021. A scenario-based approach for urban water management in the context of the COVID-19 pandemic and a case study for the Tabriz metropolitan area. Iran. Sci. Total Environ. https://doi.org/10.1016/j.scitotenv.2021.148272.

Foo, K.Y., Hameed, B.H., 2010. Insights into the modeling of adsorption isotherm systems. Chem. Eng. J. https://doi.org/10.1016/j.cej.2009.09.013.

Gautret, P., Lagier, J.C., Parola, P., Hoang, V.T., Meddeb, L., Mailhe, M., Doudier, B., Courjon, J., Giordanengo, V., Vieira, V.E., Tissot Dupont, H., Honoré, S., Colson, P., Chabrière, E., La Scola, B., Rolain, J.M., Brouqui, P., Raoult, D., 2020. Hydroxychloroquine and azithromycin as a treatment of COVID-19: results of an open-label non-randomized clinical trial. Int. J. Antimicrob. Agents. https://doi.org/10.1016/j.ijantimicag.2020.105949.

Guerra, A.C.S., de Andrade, M.B., Tonial dos Santos, T.R., Bergamasco, R., 2021. Adsorption of sodium diclofenac in aqueous medium using graphene oxide nanosheets. Environ. Technol. https://doi.org/10.1080/09593330.2019.1707882.

Hacıosmanoğlu, G.G., Doğruel, T., Genç, S., Oner, E.T., Can, Z.S., 2019. Adsorptive removal of bisphenol A from aqueous solutions using phosphonated levan. J. Hazard Mater. 374, 43–49. https://doi.org/10.1016/j.jhazmat.2019.04.015.

Han, D., Jia, W., Liang, H., 2010. Selective removal of 2,4-dichlorophenoxyacetic acid from water by molecularly-imprinted amino-functionalized silica gel sorbent. J. Environ. Sci. https://doi.org/10.1016/S1001-0742(09)60099-1.

Hiew, B.Y.Z., Lee, L.Y., Lee, X.J., Gan, S., Thangalazhy-Gopakumar, S., Lim, S.S., Pan, G. T., Yang, T.C.K., 2019. Adsorptive removal of diclofenac by graphene oxide: optimization, equilibrium, kinetic and thermodynamic studies. J. Taiwan Inst. Chem. Eng. https://doi.org/10.1016/j.jtice.2018.07.034.

Homem, N.C., Beluci, N.C.L., Amorim, S., Reis, R., Vieira, A.M.S., Vieira, M.F., Bergamasco, R., Amorim, M.T.P., 2019. Surface modification of a polyethersulfone microfiltration membrane with graphene oxide for reactive dyes removal. Appl. Surf. Sci. 486, 499–507.

Hoppen, M.I., Carvalho, K.Q., Ferreira, R.C., Passig, F.H., Pereira, I.C., Rizzo-Domingues, R.C.P., Lenzi, M.K., Bottini, R.C.R., 2019. Adsorption and desorption of acetylsalicylic acid onto activated carbon of babassu coconut mesocarp. J. Environ. Chem. Eng. 7, 102862. https://doi.org/10.1016/j.jece.2018.102862.

Hummers, W.S., Offeman, R.E., 1958. Preparation of graphitic oxide. J. Am. Chem. Soc. 80 https://doi.org/10.1021/ja01539a017, 1339–1339.
Januário, E.F.D., Beluci, N.C.L., Vidovix, T.B., Vieira, M.F., Bergamasco, R., Vieira, A.M. S., 2020. Functionalization of membrane surface by layer-by-layer self-assembly method for dyes removal. Process Saf. Environ. Protect. 134, 140–148. https://doi.org/10.1016/j.psep.2019.11.030.
Januário, E.F.D., Vidovix, T.B., Bergamasco, R., Vieira, A.M.S., 2021a. Performance of a hybrid coagulation/flocculation process followed by modified microfiltration membranes for the removal of solophenyl blue dye. Chem. Eng. Process. - Process Intensif. https://doi.org/10.1016/j.cep.2021.108577, 108577.
Januario, E.F.D., Vidovix, T.B., de Araujo, L.A., Beltran, L.B., Bergamasco, R., Vieira, A. M.S., 2021b. Investigation of Citrus reticulata peels as an efficient and low-cost adsorbent for the removal of safranin orange dye. Environ. Technol. 1–37. https://doi.org/10.1080/09593330.2021.1946601.
Januário, E.F.D., Vidovix, T.B., de Camargo Lima Beluci, N., Paixão, R.M., da Silva, L.H. B.R., Homem, N.C., Bergamasco, R., Vieira, A.M.S., 2021c. Advanced graphene oxide-based membranes as a potential alternative for dyes removal: a review. Sci. Total Environ. 789, 147957. https://doi.org/10.1016/j.scitotenv.2021.147957.
Karkooti, A., Yazdi, A.Z., Chen, P., McGregor, M., Nazemifard, N., Sadrzadeh, M., 2018. Development of advanced nanocomposite membranes using graphene nanoribbons and nanosheets for water treatment. J. Membr. Sci. 560, 97–107. https://doi.org/10.1016/j.memsci.2018.04.034.
Koch, C.C., 2007. Structural nanocrystalline materials: an overview. J. Mater. Sci. 42, 1403–1414. https://doi.org/10.1007/s10853-006-0609-3.
Langmuir, I., 1917. The constitution and fundamental properties of solids and liquids. J. Am. Chem. Soc. https://doi.org/10.1021/ja02254a006.
Li, D., Hua, T., Yuan, J., Xu, F., 2021. Methylene blue adsorption from an aqueous solution by a magnetic graphene oxide/humic acid composite. Colloid. Surfac. A Physicochem. Eng. Asp. https://doi.org/10.1016/j.colsurfa.2021.127171.
Lin, X., Huang, Q., Qi, G., Shi, S., Xiong, L., Huang, C., Chen, Xuefang, Li, H., Chen, Xinde, 2017. Estimation of fixed-bed column parameters and mathematical modeling of breakthrough behaviors for adsorption of levulinic acid from aqueous solution using SY-01 resin. Separ. Purif. Technol. https://doi.org/10.1016/j.seppur.2016.10.016.
Lladó, J., Lao-luque, C., Fuente, E., Ruiz, B., 2016. Removal of pharmaceutical industry pollutants by coal-based activated carbons. Process Saf. Environ. Protect. 104, 294–303. https://doi.org/10.1016/j.psep.2016.09.009.
Luciano, A.J.R., De Sousa Soletti, L., Ferreira, M.E.C., Cusioli, L.F., De Andrade, M.B., Bergamasco, R.N., Yamaguchi, N.U., 2020. Manganese ferrite dispersed over graphene sand composite for methylene blue photocatalytic degradation. J. Environ. Chem. Eng. https://doi.org/10.1016/j.jece.2020.104191.
Ma, J., Zhao, J., Zhu, Z., Li, L., Yu, F., 2019. Effect of microplastic size on the adsorption behavior and mechanism of triclosan on polyvinyl chloride. Environ. Pollut. https://doi.org/10.1016/j.envpol.2019.113104.
Marichelvam, M.K., Azhagurajan, A., 2018. Removal of mercury from effluent solution by using banana corm and neem leaves activated charcoal. Environ. Nanotechnol. Monit. Manag. https://doi.org/10.1016/j.enmm.2018.08.005.
Modesto, H.R., Lemos, S.G., dos Santos, M.S., Komatsu, J.S., Gonçalves, M., Carvalho, W. A., Carrilho, E.N.V.M., Labuto, G., 2021. Activated carbon production from industrial yeast residue to boost up circular bioeconomy. Environ. Sci. Pollut. Res. https://doi.org/10.1007/s11356-020-10458-z.
Nazari, G., Abolghasemi, H., Esmaieli, M., 2016. Batch adsorption of cephalexin antibiotic from aqueous solution by walnut shell-based activated carbon. J. Taiwan Inst. Chem. Eng. https://doi.org/10.1016/j.jtice.2015.06.006.
Noureddine, O., Issaoui, N., Al-Dossary, O., 2021. DFT and molecular docking study of chloroquine derivatives as antiviral to coronavirus COVID-19. J. King Saud Univ. Sci. https://doi.org/10.1016/j.jksus.2020.101248.
Paixão, R.M., Reck, I.M., Bergamasco, R., Vieira, M.F., Vieira, A.M.S., 2018. Activated carbon of Babassu coconut impregnated with copper nanoparticles by green synthesis for the removal of nitrate in aqueous solution. Environ. Technol. 39 https://doi.org/10.1080/09593330.2017.1345990, 1994–2003.
Poschet, J.F., Perkett, E.A., Deretic, V., Timmins, G., 2020. Azithromycin and ciprofloxacin have a chloroquine-like effect on respiratory epithelial cells. bioRxiv. https://doi.org/10.1101/2020.03.29.008631.
Quesada, H.B., Baptista, A.T.A., Cusioli, L.F., Seibert, D., de Oliveira Bezerra, C., Bergamasco, R., 2019a. Surface water pollution by pharmaceuticals and an alternative of removal by low-cost adsorbents: a review. Chemosphere. https://doi.org/10.1016/j.chemosphere.2019.02.009.
Quesada, H.B., Cusioli, L.F., de Oliveira Bezerra, C., Baptista, A.T.A., Nishi, L., Gomes, R. G., Bergamasco, R., 2019b. Acetaminophen adsorption using a low-cost adsorbent prepared from modified residues of Moringa oleifera Lam. seed husks. J. Chem. Technol. Biotechnol. 94, 3147–3157. https://doi.org/10.1002/jctb.6121.
Quesada, H.B., De Araújo, T.P., Cusioli, L.F., De Barros, M.A.S.D., Gomes, R.G., Bergamasco, R., 2021. Evaluation of novel activated carbons from chichá-do-cerrado (Sterculia striata St. Hil. et Naud) fruit shells on metformin adsorption and treatment of a synthetic mixture. J. Environ. Chem. Eng. https://doi.org/10.1016/j.jece.2020.104914.
Rivera-Utrilla, J., Sánchez-Polo, M., Ferro-García, M.Á., Prados-Joya, G., Ocampo-Pérez, R., 2013. Pharmaceuticals as emerging contaminants and their removal from water. A review. Chemosphere. https://doi.org/10.1016/j.chemosphere.2013.07.059.
Rostamian, R., Behnejad, H., 2018. A comprehensive adsorption study and modeling of antibiotics as a pharmaceutical waste by graphene oxide nanosheets. Ecotoxicol. Environ. Saf. https://doi.org/10.1016/j.ecoenv.2017.08.019.
Springer, V., Pecini, E., Avena, M., 2016. Magnetic nickel ferrite nanoparticles for removal of dipyrone from aqueous solutions. J. Environ. Chem. Eng. https://doi.org/10.1016/j.jece.2016.08.026.
Tran, H.N., You, S.J., Hosseini Bandegharaei, A., Chao, H.P., 2017. Mistakes and inconsistencies regarding adsorption of contaminants from aqueous solutions: a critical review. Water Res. 120, 88–116. https://doi.org/10.1016/j.watres.2017.04.014.
Vidovix, T.B., Freitas, E., Januário, D., 2019a. Bisfenol A adsorption using a low-cost adsorbent prepared from residues of babassu coconut peels. Environ. Technol. 1–13. https://doi.org/10.1080/09593330.2019.1701568, 0.
Vidovix, T.B., Quesada, H.B., Januário, E.F.D., Bergamasco, R., Vieira, A.M.S., 2019b. Green synthesis of copper oxide nanoparticles using Punica granatum leaf extract applied to the removal of methylene blue. Mater. Lett. https://doi.org/10.1016/j.matlet.2019.126685.
Vieira, A.P., Santana, S.A.A., Bezerra, C.W.B., Silva, H.A.S., Chaves, J.A.P., de Melo, J.C. P., da Silva Filho, E.C., Airoldi, C., 2009. Kinetics and thermodynamics of textile dye adsorption from aqueous solutions using babassu coconut mesocarp. J. Hazard Mater. 166, 1272–1278. https://doi.org/10.1016/j.jhazmat.2008.12.043.
Weber, W.J., McGinley, P.M., Katz, L.E., 1991. Sorption phenomena in subsurface systems: concepts, models and effects on contaminant fate and transport. Water Res. 25, 499–528. https://doi.org/10.1016/0043-1354(91)90125-A.
Weber, W.J., Morris, J.C., 1963. Kinetics of adsorption on carbon from solution. J. Sanit. Eng. Div. 89, 31–60. https://doi.org/10.1080/002689796173345.
Wernke, G., Silva, M.F., Silva, E.A. da, Fagundes-Klen, M.R., Suzaki, P.Y.R., Triques, C.C., Bergamasco, R., 2021. Ag and CuO nanoparticles decorated on graphene oxide/activated carbon as a novel adsorbent for the removal of cephalexin from water. Colloid. Surfac. A Physicochem. Eng. Asp. https://doi.org/10.1016/j.colsurfa.2021.127203.
Wu, F.C., Tseng, R.L., Juang, R.S., 2009. Initial behavior of intraparticle diffusion model used in the description of adsorption kinetics. Chem. Eng. J. https://doi.org/10.1016/j.cej.2009.04.042.
Yamaguchi, N.U., Bergamasco, R., Hamoudi, S., 2016. Magnetic MnFe2O4–graphene hybrid composite for efficient removal of glyphosate from water. Chem. Eng. J. 295, 391–402. https://doi.org/10.1016/j.cej.2016.03.051.
Yunus, A.P., Masago, Y., Hijioka, Y., 2020. COVID-19 and surface water quality: improved lake water quality during the lockdown. Sci. Total Environ. https://doi.org/10.1016/j.scitotenv.2020.139012.
Zhang, Y., Zhu, C., Liu, F., Yuan, Y., Wu, H., Li, A., 2019. Effects of ionic strength on removal of toxic pollutants from aqueous media with multifarious adsorbents: a review. Sci. Total Environ. https://doi.org/10.1016/j.scitotenv.2018.07.279.